Journal of Hazardous Materials 201–202 (2012) 125–131

Contents lists available at SciVerse ScienceDirect

Journal of Hazardous Materials

journal homepage: www.elsevier.com/locate/jhazmat

Highly efficient degradation of azo dyes by palladium/hydroxyapatite/Fe_3O_4 nanocatalyst

Afsaneh Safavi [a,b,*], Safieh Momeni [a,b]

[a] Department of Chemistry, College of Sciences, Shiraz University, Shiraz, Iran
[b] Nanotechnology Research Institute, Shiraz University, Shiraz, Iran

ARTICLE INFO

Article history:
Received 3 July 2011
Received in revised form
13 November 2011
Accepted 15 November 2011
Available online 22 November 2011

Keywords:
Magnetic nanoparticles
Palladium
Hydroxyapatite
Degradation
Azo dye

ABSTRACT

Palladium/hydroxyapatite/Fe_3O_4 (Pd/HAP/Fe_3O_4) nanocatalyst was synthesized and evaluated for its catalytic activity towards the degradation of azo dyes (methyl red, methyl orange and methyl yellow) selected as test dye species. The Pd/HAP/Fe_3O_4 was employed as a novel catalyst that offers high catalytic activity, magnetic separateability and good stability. It was found that catalytic activity of this catalyst was significantly enhanced under acidic conditions. The degradation mechanism is proposed to be due to the reaction of Pd/HAP/Fe_3O_4 with dissolved oxygen with the assistance of acid to form a Pd hydroperoxide, which oxidizes azo dyes under HAP catalysis. This in turn shows the clear importance of HAP as the support for the Pd nanocatalyst. The concentrations of dyes change exponentially with time and high rate constants were obtained for the degradation of these dyes. The pseudo-first-order equation was shown to fit degradation kinetics in most cases. Therefore, the Pd/HAP/Fe_3O_4 nanostructures are considered as a highly efficient and promising catalyst in degradation systems and they can be effectively recovered after use.

1. Introduction

Wastewaters containing dyes and organic pollutants from dyeing and finishing industry represent an increasing and worldwide environmental hazard. It has been estimated that over 15% of the total world production of dyes is lost in their synthesis and dyeing process [1]. Azo dyes are synthetic organic dyes used in large quantities in several industries such as textile, cosmetic, paper, drug and food processing. They are the largest group of synthetic colorants known and difficult to degrade by biological treatment methods due to their complex structure and their stability. Most of these dyes are carcinogenic, harmful and reduce the light penetration in aqueous systems; thus causing a negative effect on photosynthesis and are harmful to human health.

The complete removal of the pollutant from wastewater is therefore necessary and subject of widespread research. Several processes have been studied to reach partial or complete degradation of pollutant compounds such as adsorption, coagulation, biodegradation and chemical or photochemical degradation [2].

During the photocatalytic degradation process, illuminated semiconductors such as TiO_2 [3], $MnWO_4$ [4], $ZnIn_2S_4$ [5] absorb light and generates active species which lead to complete decomposition of organic pollutants or conversion into simple harmless compounds. Among semiconductors studied so far, nanosized TiO_2 has been known to be one of the best photocatalysts because of its physical and chemical stability, low cost, non-toxicity, electronic and optical properties. However, the high rate of electron–hole recombination and high band gap ($E_g > 3.2$ eV) on TiO_2 particles results in a low efficiency of photocatalysis and limits the use of sunlight or visible light as an irradiation source in photocatalytic reactions on TiO_2.

For the purpose of overcoming these limitations of TiO_2 as a photocatalyst, numerous studies have been performed such as doping metal ions into the TiO_2 lattice [6], addition of inert support [7] and doping of metal nanoparticles [8].

Advanced oxidation processes (AOPs) are becoming more important technologies for wastewater treatment. Essentially, there are three main types of AOPs, depending on the type of oxidant (oxygen, ozone, and hydrogen peroxide). The wastewater treatment by AOPs with oxygen is very expensive and usually acts under high temperatures (200–325 °C) and pressure (50–150 bar) [9]. AOP based on H_2O_2 is considered to be one of the most effective, simple and economical methods that can oxidize and degrade many organic compounds and synthetic dyes. Catalyzed,

* Corresponding author at: Department of Chemistry, College of Sciences, Shiraz University, Shiraz, Iran. Tel.: +98 711 613 7351; fax: +98 711 228 6008.
E-mail addresses: safavi@chem.susc.ac.ir, afsaneh_safavi@yahoo.com (A. Safavi).

0304-3894/$ – see front matter © 2011 Elsevier B.V. All rights reserved.
doi:10.1016/j.jhazmat.2011.11.048

uncatalyzed and photocatalyzed decomposition of hydrogen peroxide produces highly reactive species which can degrade a broad range of organic pollutants quickly and non-selectively.

Some of the AOPs based on H_2O_2 have been developed such as Fenton's reagent [10], Fe exchanged Y zeolite [11], CeO_2 doped Fe_2O_3/γ-Al_2O_3 [12], transition metal ions supported on ZrO_2 [13] metalloporphyrins [14], photo-assisted Fe(II)/H_2O_2 [15] ultrasonic irradiation/α-FeOOH/H_2O_2 [16], horseradish peroxidase/H_2O_2 [17] and UV/H_2O_2 [18].

The other pathway is reduction degradation including electroreduction and bioreduction with enzymes and microbes [19] which consists of decolorization of azo dyes by reduction of azo bond under anaerobic conditions and subsequent full mineralization by oxidation of amine under aerobic conditions. An anaerobic biodegradation of azo dyes is a relatively slow process and could be speeded up by redox mediators, like quinones and activated carbon (AC) [20,21].

Ultrasonic techniques have been proposed to treat dye wastewaters through the production of acoustic cavitation bubbles in wastewater. The violent collapse of the cavitation bubbles results in a hot spot, which has an extremely high temperature and pressure and enables to generate OH radicals. The oxidative decomposition of dyes generally proceeds via the reaction with OH radical [22,23].

Hydroxyapatite (HAP) shows photocatalytic behavior for decomposition of methyl mercaptane [24] and calmagite [25] under UV irradiation. It has been suggested that the photocatalytic activity of HAP is due to the production of sufficient amounts of $O_2^{\bullet -}$ species under UV irradiation or heat treatment. Ag–TiO_2 supported on hydroxyapatite improved its photocatalytic activity and was used as an easy and efficient system for the complete removal of bacterial pathogens in drinking water [26].

As an alternative strategy, some magnetic functionalized materials have been used as the photocatalysts in the field of degradation of organic pollutants and these magnetic photocatalysts were fabricated using the magnetic particle and photoactive material as the core and shell, respectively. Magnetic iron oxide/titania (Fe_3O_4/TiO_2) [27] and titania-coated nickel ferrite ($NiFe_2O_4/TiO_2$) photocatalysts [28] were prepared using a coating technique in which the photoactive titanium dioxide was immobilized onto the surface of magnetic nanoparticles. Fe_3O_4/hydroxyapatite (HAP) nanoparticles have been developed as a novel photocatalyst support and show superior catalytic activity in the process of the diazinon degradation under UV irradiation [29]. The effect of calcination temperature on magnetic property and photocatalytic activity of Fe_3O_4/HAP nanoparticles was investigated [30].

A chitosan-supported palladium catalyst has been reported and successfully used for the degradation of 4-nitroaniline (4-NA) [31] and chlorophenol [32] in the presence of sodium formate, where sodium formate was used as the hydrogen donor. In another work, palladium-catalyzed hydrogenation of azo compounds using recyclable polymer supported formate as the hydrogen donor produces corresponding amine(s) in excellent yields[33]. Furthermore, Pd nanoparticles prepared by using an aqueous solution of D-glucose showed good catalytic activity in the decolorization reaction of azo dyes [34]. As mentioned above, the previous reports can degrade organic pollutants in the presence of light irradiation or adulterant such as hydrogen peroxide or sodium formate.

Although some core–shell structured magnetic catalysts have received much attention, there is no research on the magnetic-hydroxyapatite-palladium composite used as catalysts, which can degrade organic pollutants. To the best of our knowledge, most of the catalysts reported to date need either addition of an adulterant or application of light irradiation, in order to act as an efficient catalyst for dyes degredation. However, the present work focuses on fabrication of Pd/HAP/Fe_3O_4 catalyst for fast degradation of azo dyes (methyl red, methyl orange and methyl yellow), without light irradiation or addition of any adulterant. Moreover, the magnetic core in the nanoparticle is useful for facilitating the separation properties of suspended particles from solution, whereas the catalytic properties of the outer Pd/HAP shell are used to destroy organic contaminants in wastewaters. Effects of variables such as initial pH, amount of catalyst and initial dye concentrations were studied. Also, we clearly demonstrate the importance of the presence of hydroxyapatite as support for the catalytic activity of Pd/Fe_3O_4 nanocatalyst. The high recyclability of the catalyst makes it ideal for practical purposes.

2. Experimental

2.1. Apparatus and reagents

All of the chemicals were analytical grade and used without further purification. Methyl red (MR), methyl orange (MO), methyl yellow (MY), ferric chloride ($FeCl_3{\cdot}6H_2O$), ferrous chloride ($FeCl_2{\cdot}4H_2O$), sulfuric acid (H_2SO_4, 98%), hydroquinone ($C_6H_6O_2$) and calcium nitrate ($Ca(NO_3)_2$) were obtained from Merck. Ammonium phosphate ($(NH_4)_2HPO_4$) and anhydrous palladium (II) chloride ($PdCl_2$) were supplied by Fluka. All the aqueous solutions of azo dyes were prepared with deionized water.

X-ray diffraction patterns of the NPs were obtained using a XRD D8, Avance, Bruker, axs. TEM images were obtained with a Philips model CM 10 transmission electron microscope. A tube furnace (Azar Furnace-Iran) equipped with gas flow line was used for thermal treatment. A Shimadzu 1601PC UV–Vis spectrophotometer (Kyoto, Japan) was used for recording the spectrophotometric data. The LC–MS system (LCMS-2010 EV Shimadzu) was equipped with Shimpack XR-ODS C18 column (5 mm × 20 mm i.d., 5 μm). Methanol–water (50/50, v/v) solution was used as a mobile phase at a flow rate of 0.2 ml min^{-1}. 5 μl of sample was injected by an autosampling device. The mass spectrometer was equipped with an electrospray ionization (ESI) source and operated in the positive ion mode. The ESI conditions were as follows: capillary voltage, 1.5 kV; gas flow, 1.5 L min^{-1} and desolvation temperature, 200 °C. The mass spectrophotometer was scanned from m/z = 100 to 400 for recording the mass spectra.

2.2. Synthesis of palladium/hydroxyapatite/Fe_3O_4

Magnetite nanoparticles (MNs) were synthesized by coprecipitation method [35]. Briefly, $FeCl_2{\cdot}4H_2O$ (2 g) and $FeCl_3{\cdot}6H_2O$ (5.2 g) were dissolved in 25 ml deionized water under nitrogen and the resulting solution was added dropwise to a 250 ml of NaOH solution (0.1 M) under vigorous mechanical stirring at 80 °C for 30 min. The magnetite precipitates were washed with deionized water and was stored in deionized water at a concentration of 10 g L^{-1}.

Hydroxyapatite nanoparticles were synthesized in the presence of Fe_3O_4 by treatment of a calcium phosphate precipitate produced at pH 10 by dropwise addition of aqueous ammonium phosphate (100 ml, 5.4 mM) to a solution containing calcium nitrate (100 ml, 9.1 mM) and magnetic nanoparticles (1 g) at a Ca^{2+}:PO_4^{3-} molar ratio of 3:1 [36]. The resulting brown solution was refluxed at 90 °C. After 2 h, the mixture was cooled to room temperature and aged overnight. The obtained precipitate was filtered, washed with deionized water till neutrality and was stored under distilled deionized water. The HAP/Fe_3O_4 (1 g) was treated with a solution of $PdCl_2$ (200 ml of 6 mM) at room temperature for 24 h and then calcined at different temperatures (50, 300, 500, 700 °C). After calcination process, palladium ions in the structure of HAP was reduced with $NaBH_4$ to produce Pd nanoparticles. Then, the mixture was separated with a magnet and washed thoroughly with distilled water and dried under

vacuum overnight. The catalyst synthesized at 300, 500, 700 °C are hereafter abbreviated as "Cat-300", "Cat-500" and "Cat-700", respectively.

2.3. Catalytic degradation of azo dyes

The catalytic activity of the Pd/HAP/Fe_3O_4 catalyst was tested for the degradation of azo dyes. The degradation of the azo dyes (MR, MO and MY) was carried out in a quartz cell with optical path length of 1 cm containing a solution of MR (0.5 mg of MR in 100 ml of 0.1 M H_2SO_4). Catalytic testing was done by the addition of the catalyst to the dye solution under ambient conditions (T 25 °C). The solution was stirred mechanically during the whole process. The decomposition of azo dyes was monitored spectroscopically with a UV–vis absorption spectrophotometer. The measurements were carried out in fast mode (350–700 nm in 30 s) in every 3–5 min interval. The nanocatalyst could be easily separated from the solution mixture by putting an external magnet into the vicinity of the cell. After complete degradation of azo dyes, the separated nanocatalyst was washed with distilled water and applied in recycling purposes. Hydroquinone solution was prepared by dissolution of 0.275 g of HQ in 25 ml of 0.1 M H_2SO_4. Effect of solution pH on the rate of degradation of azo dyes was investigated with a fixed azo dye concentration (5 μg ml^{-1}) at pH 1, 2, 7 and 10. The effect of initial dye concentrations on the degradation was investigated in 3, 5 and 7 μg ml^{-1} dye solutions. In order to know the effect of the catalyst amount on the removal of dye concentration (5 μg ml^{-1}), degradation procedure was performed with different amounts of catalyst (0, 1, 3, 5 and 10 mg) in solution.

3. Results and discussion

As explained in the experimental section, Pd/HAP/Fe_3O_4 catalyst was synthesized under different heat treating temperatures. Fig. 1 shows the XRD patterns of the HAP/Fe_3O_4 and Pd/HAP/Fe_3O_4 catalyst heat treated at 50 °C (a), 500 °C (b) and 700 °C (c). It could be seen that there are numerous sharp peaks and a low background in the XRD pattern of the HAP/Fe_3O_4 which indicate that the samples are well crystallized. The formation of Pd nanoparticles was confirmed by observation of broad peaks in the XRD spectrum (Fig. 1b). Fig. 1b shows all of the major peaks of palladium at 40 (1 1 1), 45.5 (2 0 0), 67.5 (2 2 0), 81 (3 1 1) and 86 (2 2 2) planes. Based on these observed planes, Pd nanoparticles have the face centered cubic

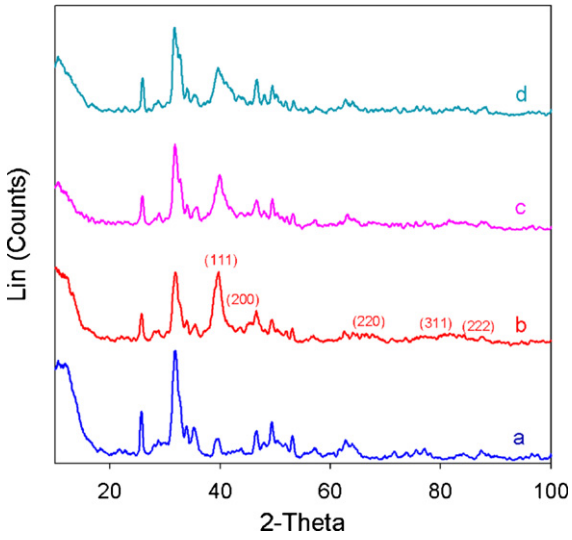

Fig. 1. XRD patterns of the as-prepared HAP/Fe_3O_4 (a) and Pd/HAP/Fe_3O_4 catalyst at (b) 50 °C, (c) 500 °C and (d) 700 °C.

crystalline structure. The width of the peaks corresponding to Pd, presents an increasing trend as the heat treatment temperature increases.

The morphology and structure of the as-synthesized Pd/HAP/Fe_3O_4 nanoparticles and its heat treated form at 500 °C are shown in the TEM images (Fig. 2). All samples display uniform HAP rod-like structures. The TEM observation revealed that the catalyst had small nano-sized particles of Pd on the rod shaped crystals of HAP. The Pd nanoparticles with a size of about 7–10 nm were clearly observed on the hydroxyapatite surface (densly distributed dark spots). When the synthesis tempreture was increased to 500 °C (Fig. 2b), the HAP crystals became larger. The mean diameters of Pd nanoparticles in the as-synthesized catalyst and heat treated form at 500 °C were 9.0 and 7.0 nm, respectively.

Fig. 3 shows the UV/vis absorption against time recorded for 4 ml of 5 μg ml^{-1} methyl red solution without any catalyst (Fig. 3a), with dispersed HAP/Fe_3O_4 (Fig. 3b) and Pd/HAP/Fe_3O_4 (Fig. 3c). No significant decrease in the intensity of the characteristic band of MR at 515 nm was observed after 90 min in the absence of the Pd and in the presence of HAP/Fe_3O_4. It is interesting to note that in contrast

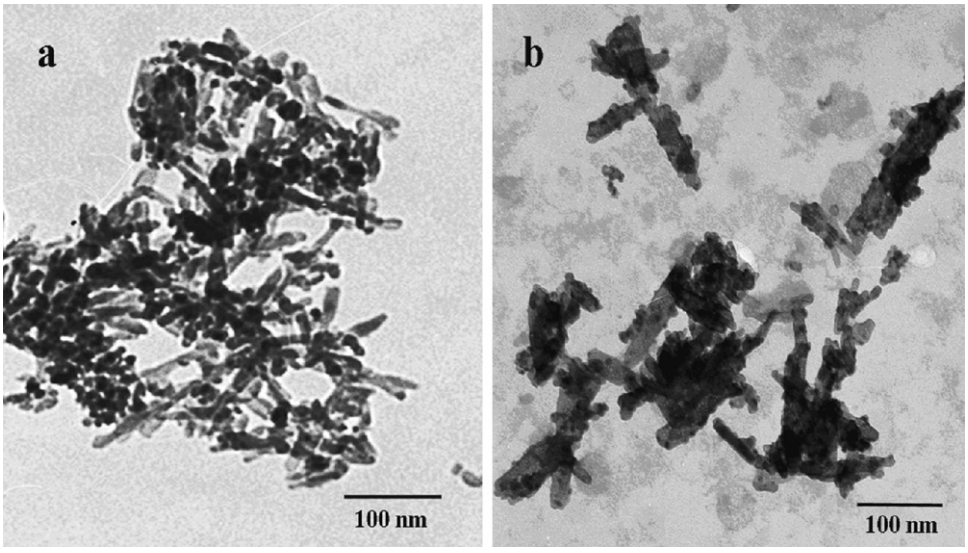

Fig. 2. TEM image of the nanosize Pd/HAP/Fe_3O_4 catalyst prepared at (a) 50 °C and (b) 500 °C.

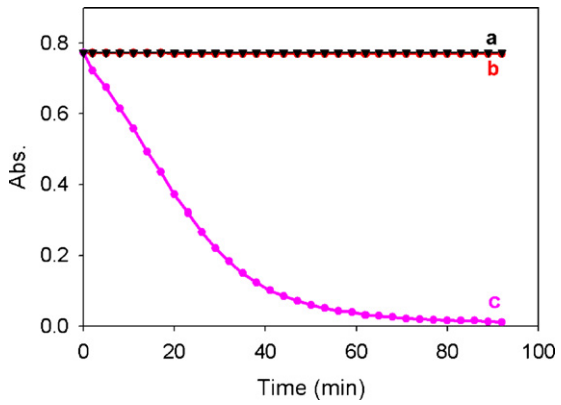

Fig. 3. Decrease in MR concentration over the time under different conditions, (a) without any catalyst (b) with HAP/Fe_3O_4 and (c) with Pd/HAP/Fe_3O_4 catalyst.

to HAP/Fe_3O_4, Pd/HAP/Fe_3O_4 catalyst effectively degrades MR. A sharp decrease of absorbance at 515 nm (Fig. 3c) shows this fact. Obviously, the MR solution can only be degraded in the presence of Pd/HAP/Fe_3O_4 catalyst under acidic conditions.

To further investigate the catalytic activity of the Pd/HAP/Fe_3O_4 catalyst, the decolorization of MR, MO and MY was tested. The decolorization was monitored by UV/vis measurements during a certain time interval. The decay of the absorbance at 515 nm for MR, 505 nm for MO and 510 nm for MY (Fig. 4) was monitored over time. MO was chosen as a simulative contaminant to evaluate the catalytic activity of Pd/HAP/Fe_3O_4. Similar to the MR results, the MO solution showed no degradation without any catalyst. UV–vis spectral changes during the catalytic degradation of MO in the aqueous Pd/HAP/Fe_3O_4 dispersion are shown in Fig. 4B. A complete decomposition of azo dyes was observed over Pd/HAP/Fe_3O_4 under acidic conditions.

The catalytic activity of Pd/HAP/Fe_3O_4 after heat treatment towards degradation of different dyes was investigated. Fig. 5 illustrates the time-dependent absorption spectra of MR aqueous solutions in the presence of Pd/HAP/Fe_3O_4 nanostructures under different heat treating temperatures (ranging from 50 to 700 °C). In the presence of Cat-500 and Cat-700, MR solution was completely degraded after 80 min, while for Cat-50, the degradation time lasted 200 min for complete removal of MR. The obtained results demonstrate that increasing the temperature (during the synthesis of catalyst) results in improvement of the catalytic activity of Pd/HAP/Fe_3O_4. It could be clearly seen that (Fig. 5), the Cat-500 and Cat-700 have the best catalytic activity towards degradation of MR. Considering the energy waste and economic reason, the catalyst synthesized at 500 °C was selected for further investigation. As suggested previously, the higher activity of the calcined catalyst in degradation process may be due to the formation of radical species in the structure of HAP [37–39].

The solution pH significantly influences the degradation of organic compounds. The results indicate that the catalytic activity of Pd/HAP/Fe_3O_4 increases with the decrease of initial pH. The catalytic experiments reveal that the decolorization efficiency of the azo dyes (5 μg ml^{-1}) on the Pd/HAP/Fe_3O_4 catalyst powder was very fast in acidic solution (pH 1), but relatively slow in neutral or basic solutions. The degradation behavior of the dyes with respect to solution pH is obvious from Table 1. The rate of degradation clearly decreased when the pH was increased from 1.0 to 7.0, indicating that the pH of the solution could influence the activity of the catalyst. Thus, the Pd/HAP/Fe_3O_4 is probably active for the degradation reaction only in acidic solutions.

More detailed information about the catalytic activity of the catalyst is demonstrated by studying the kinetics of the degradation reaction. The results show that the catalytic decolorization of

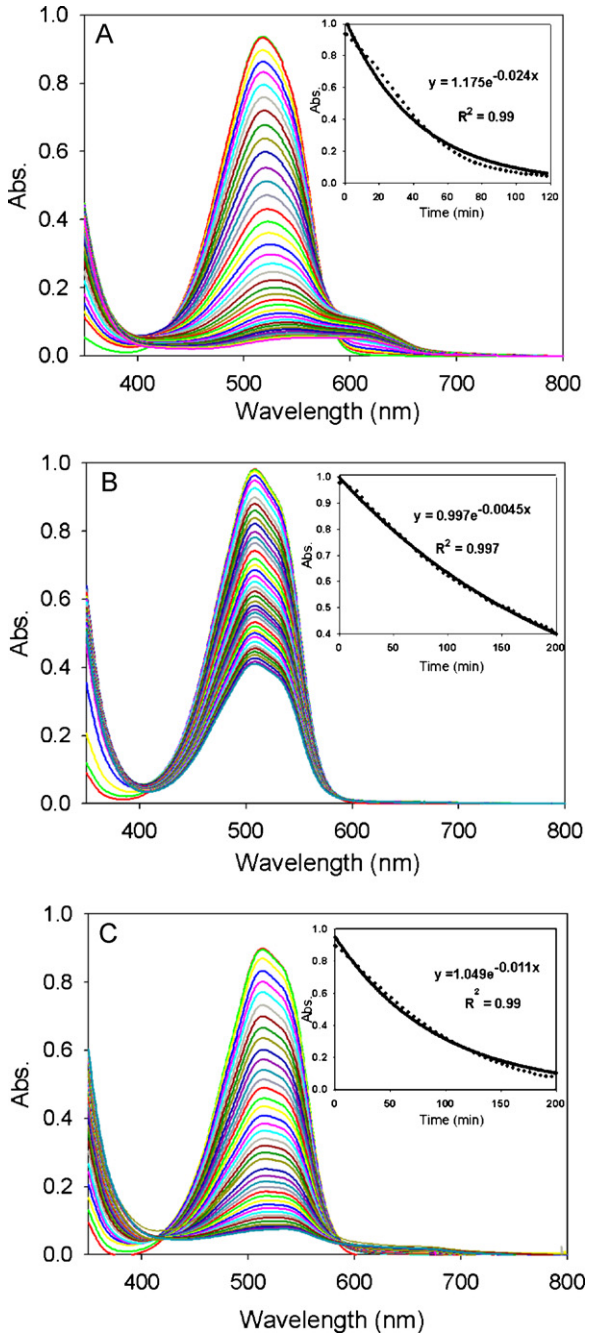

Fig. 4. Change in the absorbance spectrum, with time, during the reaction of the MR (A) MO (B) and MY (C) solution in the presence of Pd/HAP/Fe_3O_4 catalyst in 0.1 M H_2SO_4. Inset shows the absorbance decay of azo dyes with time in the presence of Pd/HAP/Fe_3O_4.

these azo dyes can be described by the first order kinetic model, $\ln(C_0/C_t) = K_t$, where C_0 is the initial concentration, C_t is the concentration at time t and K is the apparent rate constant. The rate constants for the fitted lines were calculated as 0.0385, 0.0045 and 0.0127 for MR, MO and MY, respectively.

According to the above observations, a synergistic mechanism for the azo dyes degradation in Pd/HAP/Fe_3O_4 systems is proposed. It has been reported previously that Pd can catalyze the reduction of dissolved oxygen to produce a Pd hydroperoxide under acidic conditions [40,41]. In this study, it seems that Pd hydroperoxide is a key intermediate that has been used as an oxidant in degradation reactions. To validate this hypothesis, the effect of oxygen on the degradation reaction was studied. Fig. 6 shows that, when

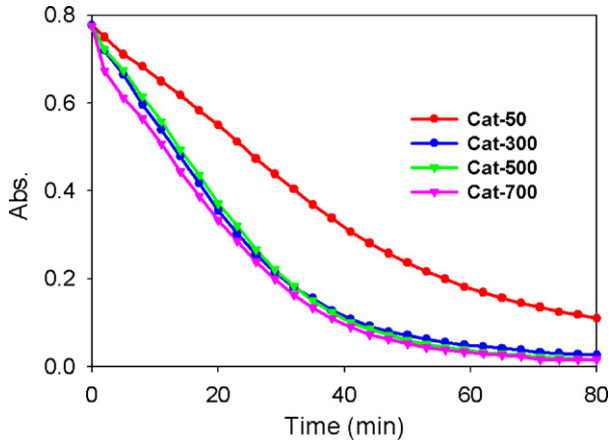

Fig. 5. Catalytic degradation of 7 μg ml^{-1} of MR by different catalysts prepared at different temperatures.

nitrogen was bubbled into the reaction system, decolorization of solution was markedly decreased, whereas decolorization of MO occurs under air. This confirms the fact that oxygen participates effectively in the degradation reaction.

Furthermore, the oxidative activity of the generated Pd hydroperoxide species as a key intermediate in the acidic Pd/HAP/Fe_3O_4 was examined. It has been reported that hydroquinone could be oxidized to p-benzoquinone with hydrogen peroxide in the presence of acrylic resin-supported Cu (II) [42] and silver oxide [43]. It is assumed that Pd hydroperoxide species might be similar to hydrogen peroxide in terms of oxidative activity. Therefore, the acidic Pd/HAP/Fe_3O_4 was used to oxidize hydroquinone to benzoquinone. Fig. 7 shows that the concentration of benzoquinone increases with time. Moreover, the Pd hydroperoxide species has stronger oxidative activity under acidic conditions [43]. This confirms the hypothesis that the acidic Pd/HAP/Fe_3O_4 can produce oxidative species.

Consequently, it seems that Pd on the surface of the hydroxyapatite reacts with dissolved oxygen under acidic conditions to yield a Pd hydroperoxide species. Earlier work has shown that Au/HAP exhibits the highest activity for oxidation of organic compounds compared to the other supports [44]. $Cu_2(OH)PO_4$ with structure similar to HAP decomposed hydrogen peroxide to generate a high concentration of hydroxyl radicals, which could be responsible for the high catalytic activity [45]. Thus, considering that the Pd hydroperoxide species in the acidic Pd/HAP/Fe_3O_4 showed properties similar to those of hydrogen peroxide, it is suggested that HAP catalyzes the degradation reaction between Pd hydroperoxide and azo dyes. The Pd-hydroperoxide species in

Table 1
Degradation of azo dyes in aqueous suspensions of Pd/HAP/Fe_3O_4 catalyst under different conditions.

Parameters		Rate constant (min^{-1})		
		MR	MO	MY
Reaction pH	1	0.0385	0.0055	0.0127
	2	0.0029	0.0011	0.0016
	7	0.00002	0.00004	0.00001
	10	0.00001	0.00004	0.00001
Catalyst concentration (g L^{-1})	0.25	0.0238	0.0020	0.0040
	0.75	0.0363	0.0026	0.0057
	1.25	0.0388	0.0033	0.0089
	2.5	0.0499	0.0045	0.0127
Dye concentration (mg L^{-1})	3	0.0485	0.0060	0.0132
	5	0.0388	0.0055	0.0127
	7	0.0376	0.0045	0.0124

Fig. 6. Effect of oxygen on the extent of degradation. Conditions: 10 μg ml^{-1} MO in 0.1 M H_2SO_4 (pH 1.0), 10 mg catalyst; Time: 2 h.

turn decomposes at the surface of HAP to generate the reactive oxygen species such as •OH radicals, which further destructs the adsorbed azo dyes and/or diffuse into the solution to attack azo dyes molecules near the catalyst/solution interface. The rate of degradation was increased by heat treatment of the nanocatalyst. The increase in rate could be due to the generation of radical species at the surface of HAP after heat treatment.

In order to know the effect of the catalyst amount on the removal of dye concentration, experiments were performed by taking MR (5 μg ml^{-1}) at its initial pH (pH 1) with different amounts of catalyst (0, 1, 3, 5 and 10 mg) in solution. Without the catalyst the degradation efficiency was very low.

The addition of Pd/HAP/Fe_3O_4 significantly enhanced the degradation of azo dyes, because an increasing amount of the catalyst results in easier generation of strong oxidizing radical species and accelerates the decomposition of azo dyes. The results are shown in Table 1. For example, when the Pd/HAP/Fe_3O_4 concentration is

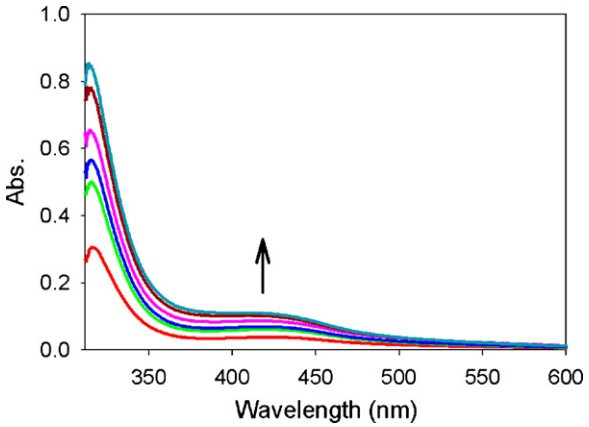

Fig. 7. Absorption spectra of the oxidation of hydroquinone mixed with acidic Pd/HAP/Fe_3O_4 colloid at different oxidation reaction stages.

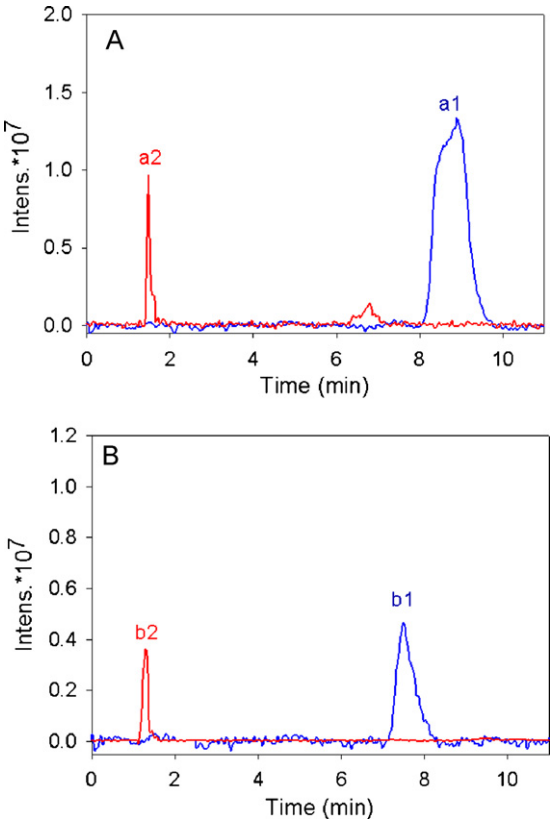

Fig. 8. LC-MS chromatograms of methyl red (A) and methyl orange (B) solutions after degradation compared to the original solutions: (a1) chromatogram of the original MR solution, $m/z = 270$; (a2) chromatogram of the MR solution after degradation $m/z = 197$, 202; (b1) chromatogram of the original MO solution, $m/z = 306$; (b2) chromatogram of the MO solution after degradation, $m/z = 196$.

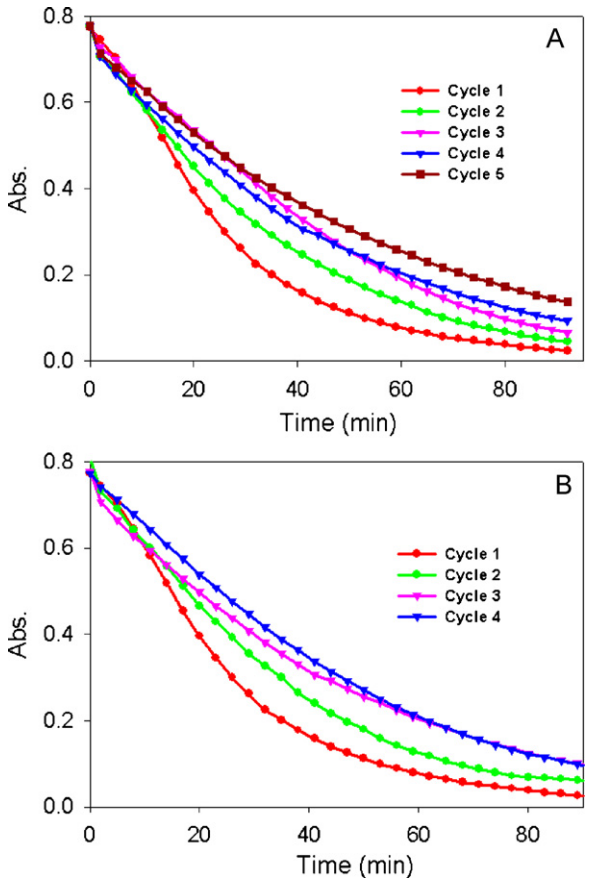

Fig. 9. Stability test on the performance of Pd/HAP/Fe_3O_4 catalyst for (A) the degradation of MR solution (5 mg L^{-1} MR in 0.1 M H_2SO_4) in five runs and (B) degradation of MR solution in wastewater; amount of catalyst; 1.25 g L^{-1}.

increased from 0.25 to 2.5 g L^{-1}, the rate constant, K, of MR degradation is greatly increased from 0.0238 to 0.0499 min^{-1}. The effect of initial dye concentrations on the degradation was investigated. As shown in Table 1, the degradation rate was decreased by increasing initial dye concentrations. This phenomenon can be explained by the fact that an increase in the initial concentration of dyes leads to an increase in the number of dye molecules. The number of radicals remains the same knowing that the concentrations of catalyst and $[H^+]$ do not change. This in turn, will cause a decrease in the kinetics and efficiency of decolorization. However, the increase in dye concentration increases the adsorption of the dye molecules on the catalyst surface, limiting the generation of radical species, and so the degradation rate decreases. Hence, the decolorization process requires more catalyst loading and longer reaction times for higher dye concentrations.

HPLC-MS analysis was applied to confirm degradation process of MR and MO at the surface of Pd/HAP/Fe_3O_4 nanocatalyst. Fig. 8 displays the chromatograms and peak intensity changes of MR and MO solutions before and after degradation processes. The peak of MR in the chromatogram appeared at 7.5 min and the intensity of the peak was 1.4×10^7 counts. After 2 h degradation, the MR peaks disappeared and two new peaks at 1.5 and 6 min ($m/z = 197$, 202) appeared. In MO solution (Fig. 8B) during the degradation prosess, the original peak at 7.5 min ($m/z = 306$) disappeared and a new peak at 1.3 min ($m/z = 196$) appeared. Based on these results, it could be concluded that some catalytic decomposition reactions have occurred in the MR and MO solution.

The recycling efficiency of the catalyst was tested by recycling the catalyst for decolorizing MR dye. Experiments were carried out for 120 min at pH 1.0 and MR concentration of 5 μg ml^{-1} (Fig. 9A). After each run, the solid powder was carefully separated from the solution by an external NdFeB strong magnet, and then rinsed by water for removing any possible remnants on the surface of the catalyst. Then, fresh MR solution was placed in the reactor using the same catalyst powder. The above catalytic process was repeated for five cycles. For the first fifth runs of the experiments, the efficiencies of all MR decolorizations were above 95%, and this indicates the efficient reusability of the catalyst. The applicability of the proposed catalyst was further evaluated by the degradation of MR in the industrial wastewater from Shiraz Industrial Complex (Shiraz, Iran). MR was spiked to the wastewater solution at the concentration level of 5 μg ml^{-1} and recycling efficiency of this catalyst was examined in wastewater. The results are demonstrated in Fig. 9B which show good degradation efficiency in sequential cycles. Thus, the proposed catalyst could be used for degradation of azo dyes in real wastewater samples.

From the economical point of view, although palladium is not considered as a cost effective catalyst but the proposed catalyst can be considered cost effective in comparison with other bulk Pd catalysts due to its nanostructure nature. In fact the weight percentage of Pd in the catalyst (Pd/HAP/Fe_3O_4) is very low. However, the main advantage of this catalyst is its ease of separation. Also, for the dye degradation process to occur, only the presence of the nanocatalyst at pH 1 is essential, and there is no need for the presence of any oxidizing or reducing agent or light irradiation.

4. Conclusions

In summary, Pd/HAP/Fe_3O_4 could degrade azo dyes under acidic conditions. The prepared nanostructures show the high catalytic

activity of Pd-HAP for the degradation of organic azo dyes without the need for visible light irradiation or application of any adulterant. More importantly, we can separate the fabricated catalyst easily from the solution by using an external magnetic field. The generation of oxidative species such as Pd-hydroperoxide at the surface of hydroxyapatite and successive oxidation reactions is proposed as the basic mechanism of this catalytic process. The importance of the support for the catalytic activity of Pd catalyst has been clearly explained. After five cycles continual utilization, this catalyst still kept high catalytic activity for degradation of the azo dyes.

Acknowledgment

The authors wish to express their gratitude to the Shiraz University Research Council for the support of this work.

References

[1] H. Wang, J. Nui, X. Long, Y. He, Sonophotocatalytic degradation of methyl orange by nano-sized Ag/TiO_2 particles in aqueous solutions, Ultrason. Sonochem. 15 (2008) 386–392.
[2] H. Zollinger, Color Chemistry, 1st ed., VCH, New York, 1987 (Chapter 16).
[3] G. Mascolo, R. Comparelli, M.L. Curri, G. Lovecchio, A. Lopez, A. Agostiano, Photocatalytic degradation of methyl red by TiO_2: comparison of the efficiency of immobilized nanoparticles versus conventional suspended catalyst, J. Hazard. Mater. 142 (2007) 130–137.
[4] H.Y. He, J.F. Huang, L.Y. Cao, J.P. Wu, Photodegradation of methyl orange aqueous on $MnWO_4$ powder under different light resources and initial pH, Desalination 252 (2010) 66–70.
[5] Z. Chen, D. Li, W. Zhang, Y. Shao, T. Chen, M. Sun, X. Fu, Photocatalytic degradation of dyes by $ZnIn_2S_4$ microspheres under visible light irradiation, J. Phys. Chem. C 113 (2009) 4433–4440.
[6] A.N. Ökte, Ö. Yılmaz, Characteristics of lanthanum loaded TiO_2-ZSM-5 photocatalysts: decolorization and degradation processes of methyl orange, Appl. Catal. A: Gen. 354 (2009) 132–142.
[7] Y.H. Chen, L.L. Chen, N.C. Shang, Photocatalytic degradation of dimethyl phthalate in an aqueous solution with Pt-doped TiO_2-coated magnetic PMMA microspheres, J. Hazard. Mater. 172 (2009) 20–29.
[8] S.K. Mohapatra, N. Kondamudi, S. Banerjee, M. Misra, Functionalization of self-organized TiO_2 nanotubes with Pd nanoparticles for photocatalytic decomposition of dyes under solar light illumination, Langmuir 24 (2008) 11276–11281.
[9] J. Levec, A. Pintar, Catalytic wet-air oxidation processes: a review, Catal. Today 124 (2007) 172–184.
[10] R.L. Kruger, R.M. Dallago, M. Di Luccio, Degradation of dimethyl disulfide using homogeneous Fenton's reaction, J. Hazard. Mater. 169 (2009) 443–447.
[11] A.K. Kondru, P. Kumar, S. Chand, Catalytic wet peroxide oxidation of azo dye (Congo red) using modified Y zeolite as catalyst, J. Hazard. Mater. 166 (2009) 342–347.
[12] Y. Liu, D. Sun, Effect of CeO_2 doping on catalytic activity of Fe_2O_3/γ-Al_2O_3 catalyst for catalytic wet peroxide oxidation of azo dyes, J. Hazard. Mater. 143 (2007) 448–454.
[13] I.A. Salem, Kinetics and mechanism of the color removal from congo red with hydrogen peroxide catalyzed by supported zirconium oxide, Transit. Metal Chem. 25 (2000) 599–604.
[14] A.C. Serra, C. Docal, A.M.D'A.R. Gonsalves, Efficient azo dye degradation by hydrogen peroxide oxidation with metalloporphyrins as catalysts, J. Mol. Catal A: Chem 238 (2005) 192–198.
[15] S.L. Orozco, E.R. Bandala, C.A. Arancibia-Bulnes, B. Serrano, R. Suárez-Parra, I. Hernández-Pérez, Effect of iron salt on the color removal of water containing the azo-dye reactive blue 69 using photo-assisted Fe(II)/H_2O_2 and Fe(III)/H_2O_2 systems, J. Photochem. Photobiol. A: Chem. 198 (2008) 144–149.
[16] M. Muruganandham, J.-S. Yang, J.J. Wu, Effect of ultrasonic irradiation on the catalytic activity and stability of goethite catalyst in the presence of H_2O_2 at acidic medium, Ind. Eng. Chem. Res. 46 (2007) 691–698.
[17] G.-Y. Kim, K.-B. Lee, S.-H. Cho, J. Shim, S.-H. Moon, Electroenzymatic degradation of azo dye using an immobilized peroxidase enzyme, J. Hazard. Mater. B126 (2005) 183–188.
[18] K. Li, M.I. Stefan, J.C. Crittenden, Trichloroethene degradation by UV/H_2O_2 advanced oxidation process: product study and kinetic modeling, Environ. Sci. Technol. 41 (2007) 1696–1703.
[19] J.P. Jadhav, G.K. Parshetti, S.D. Kalme, S.P. Govindwar, Decolourization of azo dye methyl MTCC red by Saccharomyces cerevisiae MTCC-463, Chemosphere 68 (2007) 394–400.
[20] F.P. Van der Zee, I.A.E. Bisschops, G. Lettinga, J.A. Field, Activated carbon as an electron acceptor and redox mediator during the anaerobic biotransformation of azo dyes, Environ. Sci. Technol. 37 (2003) 402–408.
[21] G. Mezohegyi, A. Kolodkin, U.I. Castro, C. Bengoa, F. Stuber, J. Font, A. Fabregat, Effective anaerobic decolorization of azo dye acid orange 7 in continuous upflow packed-bed reactor using biological activated carbon system, Ind. Eng. Chem. Res. 46 (2007) 6788–6792.
[22] K. Okitsu, K. Iwasaki, Y. Yobiko, H. Bandow, R. Nishimura, Y. Maeda, Sonochemical degradation of azo dyes in aqueous solution: a new heterogeneous kinetics model taking into account the local concentration of OH radicals and azo dyes, Ultrason. Sonochem. 12 (2005) 255–262.
[23] M. Li, J.-T. Li, H.-W. Sun, Decolorizing of azo dye reactive red 24 aqueous solution using exfoliated graphite and H_2O_2 under ultrasound irradiation, Ultrason. Sonochem. 15 (2008) 717–723.
[24] H. Nishikawa, K. Omamiuda, Photocatalytic activity of hydroxyapatite for methyl mercaptane, J. Mol. Catal. A: Chem. 179 (2002) 193–200.
[25] M.P. Reddy, A. Venugopal, M. Subrahmanyam, Hydroxyapatite photocatalytic degradation of calmagite (an azo dye) in aqueous suspension, Appl. Catal. B: Environ. 69 (2007) 164–170.
[26] M.P. Reddy, A. Venugopal, M. Subrahmanyam, Hydroxyapatite-supported Ag–TiO_2 as *Escherichia coli* disinfection photocatalyst, Water Res. 41 (2007) 379–386.
[27] D. Beydoun, R. Amal, G. Low, S. McEvoy, Occurrence and prevention of photodissolution at the phase junction of magnetite and titanium dioxide, J. Mol. Catal. A: Chem. 180 (2002) 193–200.
[28] S. Rana, R.S. Srivastava, M.M. Sorensson, R.D.K. Misra, Synthesis and characterization of nanoparticles with magnetic core and photocatalytic shell: anatase TiO_2–$NiFe_2O_4$ system, Mat. Sci. Eng. B 119 (2005) 144–151.
[29] Z.-P. Yang, X.-Y. Gong, C.-J. Zhang, Recyclable Fe_3O_4/hydroxyapatite composite nanoparticles for photocatalytic applications, Chem. Eng. J. 165 (2010) 117–121.
[30] Y. Liu, H. Zhong, L. Li, C. Zhang, Temperature dependence of magnetic property and photocatalytic activity of Fe_3O_4/hydroxyapatite nanoparticles, Mater. Res. Bull. 45 (2010) 2036–2039.
[31] T. Vincent, F. Peirano, E. Guibal, Chitosan supported palladium catalyst. VI. Nitroaniline degradation, J. Appl. Polym. Sci. 94 (2004) 1634–1642.
[32] T. Vincent, S. Spinelli, E. Guibal, Chitosan-supported palladium catalyst. II. Chlorophenol dehalogenation, Ind. Eng. Chem. Res. 42 (2003) 5968–5976.
[33] K. Abiraj, G.R. Srinivasa, D.C. Gowda, Palladium-catalyzed simple and efficient hydrogenative cleavage of azo compounds using recyclable polymer-supported formate, Can. J. Chem. 83 (2005) 517–520.
[34] L. Xu, X.C. Wu, J.J. Zhu, Green preparation and catalytic application of Pd nanoparticles, Nanotechnology 19 (2008) 305603.
[35] P. Berger, N. Adelman, K. Beckman, Preparation and properties of an aqueous ferrofluid, J. Chem. Ed. 76 (1999) 943–948.
[36] K. Mori, S. Kanai, T. Hara, T. Mizugaki, K. Ebitani, K. Jitsukawa, K. Kaneda, Development of ruthenium-hydroxyapatite-encapsulated superparamagnetic γ-Fe_2O_3 nanocrystallites as an efficient oxidation catalyst by molecular oxygen, Chem. Mater. 19 (2007) 1249–1256.
[37] Y. Matsumura, H. Kanai, J.B. Maffat, Formation of radical oxygen species on hydroxyapatite, J. Mol. Catal. A: Chem. 15 (1997) L229–L232.
[38] H. Monma, S. Ueno, T. Kanazawa, Properties of hydroxyapatite. Prepared by the hydrolysis of tricalcium phosphate, J. Chem. Tech. Biotechnol. 31 (1981) 15–24.
[39] H.C. Zhao, X.D. Li, J.X. Wang, S. Qu, J. Weng, X. Zhang, Characterization of peroxide ions in hydroxyapatite lattice, J. Biomed. Mater. Res. 52 (2000) 157–163.
[40] N. Li, W. Wang, D. Tian, H. Cui, pH-dependent catalytic properties of Pd-Ag nanoparticles in luminol chemiluminescence, Chem. Commun. 46 (2010) 1520–1522.
[41] S. Chowdhury, I. Rivalta, N. Russo, E. Sicilia, Theoretical investigation of the mechanism of acid-catalyzed oxygenation of a Pd(II)-hydride to produce a Pd(II)-hydroperoxide, J. Chem. Theory Comput. 4 (2008) 1283–1292.
[42] I. Owsik, B. Kolarz, The oxidation of hydroquinone to p-benzoquinone catalysed by Cu(II) ions immobilized on acrylic resins with aminoguanidyl groups, J. Mol. Catal. A 178 (2002) 63–71.
[43] F. Derikvand, F. Bigi, R. Maggi, C.G. Piscopo, G. Sartori, Oxidation of hydroquinones to benzoquinones with hydrogen peroxide using catalytic amount of silver oxide under batch and continuous-flow conditions, J. Catal. 271 (2010) 99–103.
[44] Y.F. Han, N. Phonthammachi, K. Ramesh, Z. Zhong, T. White, Removing organic compounds from aqueous medium via wet peroxidation by gold catalysts, Environ. Sci. Technol. 42 (2008) 908–912.
[45] Y. Zhana, H. Li, Y. Chen, Copper hydroxyphosphate as catalyst for the wet hydrogen peroxide oxidation of azo dyes, J. Hazard. Mater. 180 (2010) 481–485.